PREDICTING INTERNAL RED OAK (*QUERCUS RUBRA*) LOG DEFECT FEATURES USING SURFACE DEFECT MEASUREMENTS

R. Edward Thomas[1]

Abstract.—Determining the defects located within a log is crucial to understanding the tree/log resource for efficient processing. However, existing means of doing this non-destructively requires the use of expensive x-ray/CT (computerized tomography), MRI (magnetic resonance imaging), or microwave technology. These methods do not lend themselves to fast, efficient, and cost-effective analysis of logs and tree stems in the mill. This study quantified the relationship between external defect indicators and internal defect characteristics for red oak logs. A series of models was developed to predict internal features using visible external features: surface indicator width, length, rise, and log diameter. Good correlations and small prediction errors were observed with sound (sawn), overgrown, and unsound knot defects. For less severe defects such as adventitious buds/clusters and distortion-type defects, weaker correlations were observed, but the magnitude of prediction errors was small and acceptable.

INTRODUCTION

One of the major emphasis areas today in hardwood research is the development of equipment and a methodology to accurately sense internal defect location and structure. Determining the location and characteristics of defects located inside logs promises to dramatically improve log recovery in terms of both quantity and quality (Steele et al. 1994). In addition, accurate internal defect information would permit researchers to analyze, refine, and expand log grading rules, multi-product potential, stand differences, and impact of silvicultural treatments on quality in ways previously not available or economically feasible. The goal of this research is to provide a mathematical method of predicting internal defect size and location based on external surface indicators. This study was limited to the most common defect types that have the greatest impact on hardwood quality (tree or lumber grade).

Although there are many benefits to determining internal log information, an inexpensive and efficient method of obtaining these data does not exist today. Researchers are currently examining various approaches to this problem including the use of x-ray/CT (computerized tomography), ultrasound, MRI (magnetic resonance imaging), or radar technology (Chang 1992). Some high-volume softwood lumber mills in Europe and the Pacific Northwest have installed three-head x-ray scanners. This type of scanner uses three or four x-ray transmitters and detectors to capture internal log defect data. Although these types of scanners operate much faster than CT scanners, they obtain lower quality/resolution data. Although x-ray/CT and MRI methods show promise, the technology is prohibitively expensive and does not permit fast, efficient analysis of logs and tree stems. Both CT and three-head x-ray systems are still being used only on smaller diameter logs due to energy level issues.

Researchers have studied the relationships among surface indicators and internal defect manifestation in depth for various hardwood and softwood species. Schultz (1961), in examining German beech (*Fagus sylvatica*), found that the ratio of the bark distortion width to bark distortion length in this species is the same as the ratio of the stem when the branch was completely healed over to the current

[1]Research Scientist, U.S. Forest Service, Northern Research Station, 241 Mercer Springs Rd., Princeton, WV 24740. To contact, call 304-431-2324 or email at ethomas@fs.fed.us.

stem diameter. However, for species with heavier irregular bark, such as hard maple, he found that it was difficult to judge the clear area above the defect in this manner.

Hyvärinen (1976) explored the relationships among the internal features of grain orientation and height of clear wood above an encapsulated knot defect and the external features of surface rise, width, and length for sugar maple (*Acer saccharum*). The sugar maple defect data were collected from 44 trees obtained from three sites in upper Michigan. Hyvärinen used simple linear regression methods to find good correlations among clear wood above defects, bark distortion width, length, and rise measurements, as well as age, tree diameter, and stem taper. The best simple correlation was with diameter inside bark (DIB) ($r = 0.66$) and a 0.66-inch standard error of estimate. Correlation was further improved by using a stepwise regression method. The final model ($r = 0.74$) used bark distortion vertical size and DIB as the most significant predictor variables for predicting encapsulation depth.

A similar study was conducted on a sample of 21 black spruce (*Picea mariana*) trees collected from a natural stand 75 km north of Quebec City (Lemieux et al. 2001). Three trees, each with three logs, were selected from which a total of 249 knot defects were dissected and their data recorded. The researchers found better correlations between external indicator and internal characteristics in the middle and bottom logs as compared to the upper logs. Strong correlations ($r > .89$) were found among the length and width of internal defect zones and external features such as branch stub diameter and length. The defects were modeled as having three distinct zones corresponding to the manner in which the penetration angle changes over time in black spruce. The penetration angle is the angle at which a line through the center of the defect intersects the log surface.

Carpenter's (1950) examination of surface indicators found that although the frequency and occurrence of surface indicators within a given species vary by region, in general the same indicator will be found with its defect in the underlying wood. Thus, although certain defect types may be more prevalent in some regions, the underlying manifestation of the defect would remain more or less consistent across regions. Further, growth rate will vary from region to region (or site to site within the same region), so the defect encapsulation rate will differ also. However, the rate at which the encapsulation occurs and the degree to which the defect is occluded or covered over by clear wood are indicated in the bark pattern. Shigo and Larson (1969) discovered that the ratio of defect height to width is a strong indicator of defect depth with respect to the radius of the stem at the defect (Fig. 1). The faster the diameter growth, the faster the defect is encapsulated and the faster the bark distortion pattern changes.

More recently, the relationships among external defect indicators and internal features were examined for yellow-poplar *(Tulipifera liriodendron*) (Thomas 2008). This study found statistically significant correlations between external indicators and internal features. The strongest correlations occurred with the most severe defect types, i.e., overgrown knots, overgrown knot clusters, sound knots, and unsound knots. These defects are the most recent and therefore the least occluded. In almost all cases, the correlations observed with the severe defect types were significant ($\alpha < 0.01$). Conversely, the weakest correlations involved the least severe and most occluded defect types, i.e., adventitious knots, adventitious knot clusters, light distortions, and medium distortions. In several cases, the correlations between external and internal features failed to be statistically significant ($\alpha < 0.01$) for the less severe defect types.

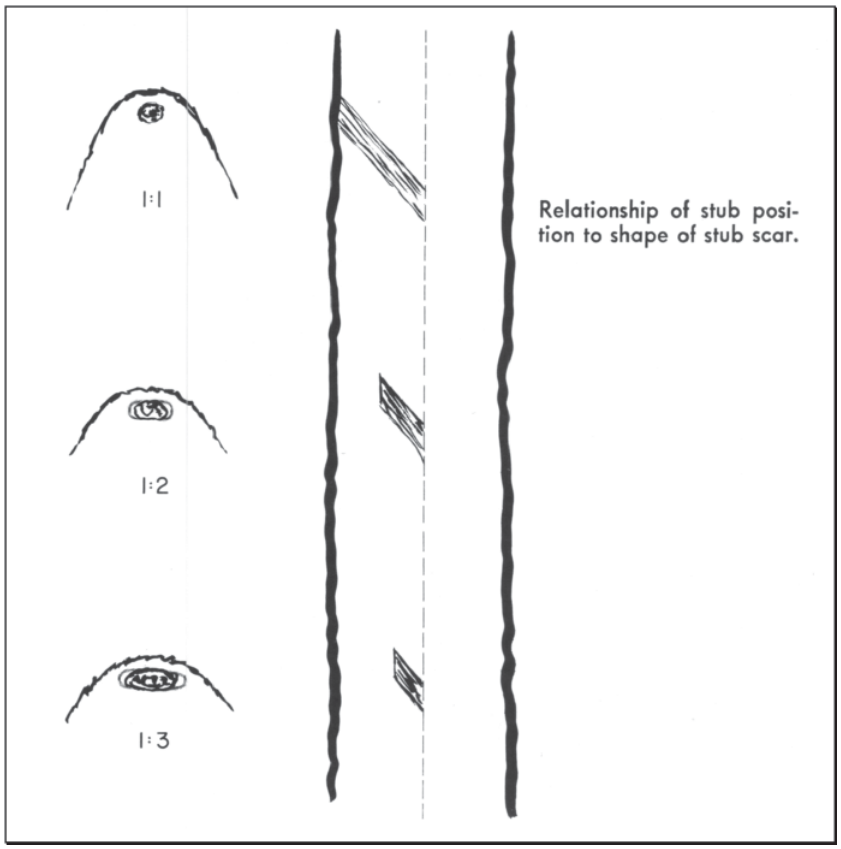

Figure 1.—Encapsulation depth and stub scar relationship ratio (Shigo and Larson 1969).

METHODS

Sample Collection

Red oak (*Quercus rubra*) defect samples were collected from two sites in West Virginia: West Virginia University Forest (WVUF) near Morgantown (elevation: 2,300 feet) and the Mead Westvaco Forest (MWF) near Rupert (elevation: 3,200 feet). The two sites are separated by about 125 miles. From each site, 33 trees were randomly selected. For each tree the number of defects by type was counted. The counts were used to develop a random sampling plan. The goal was to collect four defects of each type from each tree, whenever possible. For example, if there were eight sound knots on the tree, every second sound knot was selected. Of course, not all trees have four defects of every type. In other cases, selecting one defect would prevent another from being selected due to defect overlap. In these cases, preference went to the least common defect type on that tree and a different occurrence of the second defect type was used. The number of defect samples obtained from each site by defect type is shown in Table 1. In most cases, approximately equal numbers of each type of defect were obtained from each site.

Sample Processing

All defects were identified according to the characteristics as defined in Defects in Hardwood Timber (Carpenter et al. 1989). Once a defect was located and classified, the section containing the defect was cut from the log. The defect sections ranged from 12 to 24 inches in length. If, upon dissection, the inner portion of the defect was not completely contained within the section, the sample was

Table 1.—Types and numbers of defects collected by site and overall

Defect type	Location		Total
	WVU Forest	Mead Westvaco Forest	
Adventitious Knot (AK)	54	51	105
Adventitious Knot Cluster (AKC)	27	47	74
Heavy Distortion (HD)	52	46	98
Light Distortion (LD)	2	37	39
Medium Distortion (MD)	70	63	133
Overgrown Knot (OK)	45	114	159
Overgrown Knot Cluster (OKC)	0	48	48
Sound Knot (SK)	19	36	55
Sound Knot Cluster (SKC)	1	13	14
Unsound Knot (UK)	30	31	61
Unsound Knot Cluster (UKC)	0	13	13
Wound (WND)	0	43	43
Total	300	542	842

discarded. For each sample the following information was recorded: defect type, surface width (across grain) and length (along grain), growth rate (rings per inch), and bark thickness. The sample was then sawn into 1-inch-thick slices. This resulted in a photo series showing the defect penetrating the log (Fig. 2). For each slice, the depth, defect width, length, and distance of defect center to notch bottom center were recorded. When a defect terminated between slices, it was assumed that it terminated at the halfway point through the slice.

Modeling Statistics

A series of chi-squared tests was used to test for outliers in the internal/external dataset (Komsta 2006) Data identified by the tests as outliers were examined and corrected if in error by remeasuring the sample. The data were grouped by defect type. With the R statistical analysis program, stepwise muliple-linear regression analyses were used to test for correlations among surface indicators and internal features (R Development Core Team 2006). The independent variables used were surface indicator width (SWID), length (SLEN), rise (SRISE), and log diameter inside bark (DIB). These variables were selected because they are measurable during log surface inspection. Area (SWID * SLEN), $SLEN^2$, and $SWID^2$ also were examined as potential predictor variables. The dependent variables selected were (1) rake (penetration angle), (2) clear wood above defect, (3) total depth, (4) halfway-point cross-section width (HWID), and (5) halfway-point cross-section length (HLEN). These variables permit an internal model of a defect to be constructed and determine an approximate internal location (Fig. 3).

Within each defect type class, the data was randomly partitioned into two groups using the caTools package (Tuszynski 2006) for R. The first group contains approximately 66.7 percent of the records and was used for model development and determining the internal/external feature correlation statistic. The second set contained the remaining records and was used for testing the prediction models (model validation set). Table 2 shows the numbers of observations used in the model development and testing steps.

Figure 2.—Series of internal defect sections for a heavy distortion defect surface indicator.

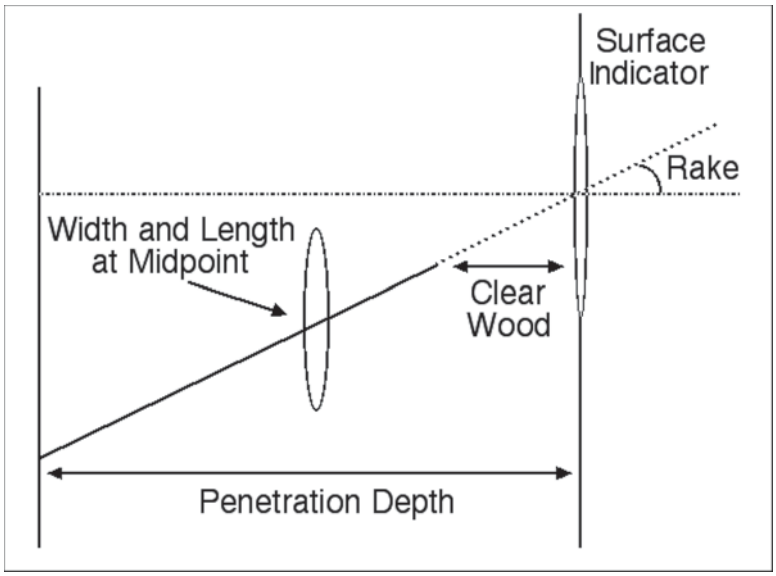

Figure 3.—Illustration of internal features predicted by the model.

Table 2.—Numbers of observations used in model development and testing by defect type

Defect type	Number of observations		Total observations
	Model dataset	Testing dataset	
AK	70	35	105
AKC	49	25	74
HD	65	33	98
LD	26	13	39
MD	88	45	133
OK	105	54	159
SK	37	18	55
UK	40	21	61
OK/SK/UK	182	93	275
OKC/SKC/UKC	46	25	71
Total	708	362	1,070

RESULTS

Correlation results for model development and significant predictor variables are presented in Table 3. A significance level of 1 percent was used for all tests. Table 3 has two major sections: model development and model testing. In each section, the correlation coefficient, significance, and the mean-absolute error (MAE) of the correlation are reported. MAE is the mean of the absolute value of the residual errors for the fitted equation. MAE indicates the +/- error range that can be expected using the fitted equation to predict defect features.

Knot Defects

Model development with the severe knots, OK, SK, and UK, discovered strong significant correlations ($\alpha < 0.01$) in almost all instances (Table 3). The exception was with overgrown knots and predicting clear area (Clear) above the encapsulated defect. Clear area above an encapsulated knot defect occurred in only a few samples, so it was weakly correlated with external features. The strength of the relationship (multiple adjusted R^2) among interior halfway point cross-section width (HWID) measurement and external features ranged from 0.53 to 0.74. Similar results were found among external features and the halfway point cross-section length (HLEN) measurement with adjusted multiple R^2 values ranging from 0.40 to 0.87. The correlation of total defect penetration depth (DEPTH) to external features ranged between 0.40 and 0.63, which was not as strong as the correlations observed with yellow-poplar, which ranged from 0.63 to 0.73 (Thomas 2008). In many cases, the defects in the samples terminated before reaching the pith, indicating an adventitious knot. This decreased the significance of DIB as a predictor variable for depth. The correlations (adjusted multiple R^2) among external features and penetration angle (RAKE) ranged from 0.39 to 0.54.

Table 3 lists the most significant independent or predictor variables for each defect type and internal feature. The independent variables are listed in the order of most to least significant. The number of instances where correlations with DIB, SLEN, and SWID were significant was nearly identical at 11, 11, and 12 instances, respectively. Interaction terms had the strongest correlation with internal features in 9 instances while non-interaction terms were the most significant in 12 instances. Correlations involving SWID and SLEN were the most common interaction terms, having a statistically significant correlation six times each. Similarly, SWID and SLEN were the most significant single independent variables, statistically significant five and four times each, respectively. Thus, with the severe knots and knot clusters, most of the strongest correlations to internal features are with the surface width and length of the defect.

The associated MAEs with the model development samples were small in most cases. The MAE values in Table 3 are reported in inches for all measurements except rake angle, which is in degrees. In 10 out of 16 cases for the knot defects, the MAE is 0.75 inch or less. In five instances, the MAE is less than 0.50 inch. In the remaining six cases, four are less than 1 inch and two are 1.15 and 1.05 inches. The MAE values for rake angles ranged between 9 and 12 degrees.

The model testing samples were used to analyze the models' predictive capabilities. The regression equations generated with the model development samples were used to predict internal feature measurements. The correlation coefficient r, the mean absolute error (MAE), and the significance level of the correlation were determined for each defect type and feature combination (Table 3). In

Table 3.—Model development and testing correlation results

		Model Development Results				Model Testing Results		
Defect type	Dependent variable	Multiple adjusted R^2	Mean absolute error	Correlation significant	Significant independent variables	Correlation coefficient 'R'	Mean absolute error	Correlation significant
AK	Hwid	0.15	0.27	Yes	slen	0.52	0.26	Yes
	Hlen	0.26	0.28	Yes	swid, slen, swid*slen, srise*slen	0.32	0.41	No
	Rake	0.12	5.04	Yes	slen, srise, srise*swid	0.51	0.83	Yes
	Depth	0.24	1.45	Yes	dib, swid, slen, srise	0.35	1.57	No
	Clear	0.10	1.27	No	srise, dib	0.40	0.93	No
AKC	Hwid	0.11	0.56	No	swid, srise	0.61	0.82	Yes
	Hlen	0.36	0.43	Yes	slen, swid*srise, slen*srise	0.33	0.81	No
	Rake	0.20	7.15	Yes	swid*srise, srise*dib	0.12	0.95	No
	Depth	0.26	1.35	Yes	dib	0.80	0.90	Yes
	Clear	0.06	1.12	No	srise	0.37	1.04	No
HD	Hwid	0.55	0.20	Yes	dib, swid, slen, dib*swid	0.43	0.28	Yes
	Hlen	0.47	0.43	Yes	slen, dib, dib*swid	0.47	0.44	Yes
	Rake	0.40	9.29	Yes	dib, slen	0.68	8.54	Yes
	Depth	0.27	0.86	Yes	dib, swid	0.51	0.72	Yes
	Clear	0.08	0.67	No	swid, slen, swid*slen	0.31	0.62	No
LD	Hwid	0.19	0.27	No	dib, slen	0.46	0.41	No
	Hlen	0.34	0.65	Yes	slen, srise	0.25	1.09	No
	Rake	0.03	10.06	No	dib, dib*swid	0.14	14.71	No
	Depth	0.09	1.05	No	dib, swid, srise	0.39	1.18	No
	Clear	0.08	0.94	No	slen	0.01	1.00	No
MD	Hwid	0.13	0.24	Yes	swid, slen, swid*slen	0.56	0.29	Yes
	Hlen	0.23	0.34	Yes	swid,dib, swid*slen, dib*slen	0.61	1.78	Yes
	Rake	0.10	10.50	Yes	dib, swid	0.46	9.92	Yes
	Depth	0.16	0.80	Yes	dib, swid	0.63	0.75	Yes
	Clear	0.10	0.86	Yes	dib, swid	0.17	1.09	Yes
OK	Hwid	0.53	0.29	Yes	dib, slen, swid*srise, slen*srise	0.46	0.40	Yes
	Hlen	0.40	0.67	Yes	slen, srise*swid, slen*srise	0.44	0.81	Yes
	Rake	0.42	10.23	Yes	dib, slen, srise, dib*srise	0.60	11.82	Yes
	Depth	0.45	0.96	Yes	dib, dib*swid	0.62	0.88	Yes
	Clear	0.03	0.04	No	swid, srise, swid*srise*slen	0.17	0.04	No
SK	Hwid	0.65	0.38	Yes	swid*slen, swid*dib	0.50	0.75	No
	Hlen	0.66	0.55	Yes	swid, srise, srise*slen, swid*srise*slen	0.61	0.71	
	Rake	0.45	9.18	Yes	dib, swid, swid*slen	0.07	19.59	No
	Depth	0.58	0.98	Yes	slen, swid, swid*dib, slen*dib	0.52	1.45	No
	Clear	--	--	No	--	--	--	No
UK	Hwid	0.74	0.30	Yes	slen, slen*swid, slen*srise, slen*dib, slen*swid*srise	0.08	0.77	No
	Hlen	0.87	0.74	Yes	swid, slen, swid*srise, swid*slen*srise	0.37	1.85	No
	Rake	0.54	10.29	Yes	swid, swid*dib	0.55	12.22	Yes
	Depth	0.63	0.72	Yes	dib, swid, slen, swid*slen, dib*slen	0.45	1.13	No
	Clear	--	--	No	--	--	--	No

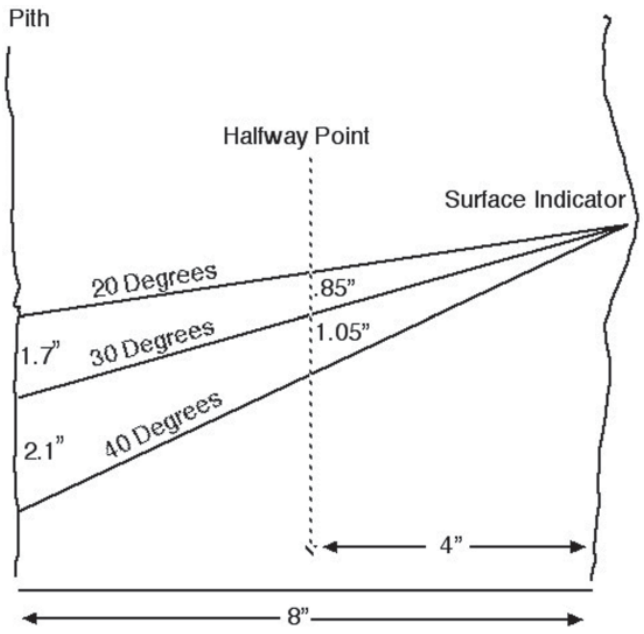

Figure 4.—Impact of rake error on internal defect position.

13 out of 21 instances, the correlation coefficients R were significant ($\alpha < 0.01$). In six instances, the correlation was not significant with the sound and unsound knots. Here the problem was due to sample size, with only 18 and 21 model testing samples for sound and unsound knots, respectively. Similarly, the low numbers of clustered knots, OKC, SKC, and UKC, prevented any analyses by individual type, and these data were not examined.

Overall, the highest correlation coefficients (R) occurred with overgrown knot samples. For all severe knot defects, HWID had the smallest MAE, ranging from 0.29 to 0.41 inch. The MAE for the predicted HLEN values also was acceptable and ranged from 0.71 to 0.81 inch where the correlation was significant. The MAE with predicted depth was lowest with overgrown knots with a value of 0.88 inch. Except for sound knots, where the correlation was not significant, the MAE for RAKE was similar with values of 11.82 to 12.22 degrees. For a 16-inch diameter log with a defect terminating near the center, a 10-degree error would change the defect center position by 1.7 (10 degrees under estimate) to 2.1 inches (10 degrees over estimate) at the pith, depending on degree (Fig. 4). The difference in defect position at the halfway point would have a maximum positional variance of 0.85 (10 degrees underestimate) to 1.05 inches (10 degrees overestimate) depending on degree.

Bark Distortion Defects

In general, the correlations between external indicator measurements and internal features for bark distortion defects (LD, MD, and HD) were not as strong as those measured for the knot defects. Distortion defects are smaller and have been encapsulated longer than the more recent knot defects. Thus, less surface information is available for these defect types. The model development correlation results for bark distortions are given in Table 3.

The strongest correlations between external and internal features for the minor defects were with the heavy distortion (HD) defect type. In most cases, a heavy distortion is an overgrown knot that has been encapsulated or overgrown to the point where it no longer has any associated surface rise. Thus, it is the youngest of the distortion defects and has the most surface detail present. The correlation

(multiple adjusted R^2) of surface features to HWID was comparable to overgrown knots (HD R^2 = 0.55 versus OK R^2 = 0.53, $\alpha < 0.01$). Similarly, the correlation with HLEN, R^2 = 0.47, was also significant and similar to that of overgrown knots, R^2 = 0.40. The MAE values for the HWID, HLEN also were acceptable at 0.20 and 0.43 inch. The other correlations for the other HD internal defect features also were significant and similar to that of the overgrown knots, with the exception of encapsulation depth (CLEAR). The MAE for penetration depth (DEPTH) was 0.86 inch and the MAE for RAKE was 9.29 degrees.

The correlations among external and internal features for the medium distortion defects were statistically significant ($\alpha < 0.01$). Although significant, the correlations were not strong. Adjusted multiple R^2 values for the internal features ranged from 0.10 to 0.23. Thus, only a fraction of the variability of the internal features can be explained by this approach. With the light distortion defects, the correlations became weaker and only the correlation with HLEN was significant with a multiple adjusted R^2 value of 0.34.

Analyzing the predictor equations for the model testing samples showed that the models developed for the HD and MD perform well. For these defects only the CLEAR correlation for heavy distortions failed to be statistically significant ($\alpha< 0.01$). The relationship (correlation coefficient R) for halfway-in-width for the HD and MD defects was 0.43 and 0.46 with MAE values of 0.28 and 0.29 inch, respectively. Although the correlations for HD and MD were stronger for HLEN, R=0.44 and R=0.61, respectively when compared to HWID, the MAE increased to 0.44 and 1.78 inches. Note that the model prediction results are nearly the same as the model development results for the MD model development results (Table 3), indicating the adequacy of the models for predicting internal feature size and location.

For the light distortions, none of the prediction models had a significant correlation to the internal features. This is likely due to the small number, 39 total, of light distortion defects. To try to improve the model's predictive ability for LD defects, the HD, MD, and LD data were grouped together and analyzed. This resulted in a larger sample of distortion defects, 177 samples for model development and 91 samples for model testing. However, the correlations between external indicators and internal features were much weaker with higher MAE values than the HD, MD, and LD models individually. From this test, it can be deduced that the classification of distortion defects has a significant impact on the application of the prediction models.

SLEN was the most common, most significant independent variable with 7 occurrences in the prediction models. SWID and DIB were the next most significant terms in 4 and 3 instances, respectively. However, DIB and SWID were the most common overall, occurring in 11 and 9 instances, respectively compared to the 8 instances with SLEN. In addition, the DIB*SWID interaction term was the most significant variable in one instance and a significant variable three other times.

Adventitious Knot Defects

Multiple adjusted R^2 for AK defects ranged from 0.12 to 0.26 for the correlations that were statistically significant ($\alpha < 0.01$). In addition, the MAE values for the HWID and HLEN internal features were 0.14 and 0.15 inch. However, for AK defects, the correlation between the clear area

above the defect and external indicators was not statistically significant ($\alpha < 0.01$). Multiple adjusted R^2 for the significant correlations with AKC defect features ranged from 0.20, for the rake angle, to 0.26 and 0.36 for the DEPTH and HLEN features. CLEAR was not significantly correlated to any external feature measurement.

The development dataset correlations for AK and AKC defects were not exceptionally strong. However, except for encapsulation depth, the MAE was small and acceptable. The MAE for penetration angle ranged from 5.04 to 7.15 degrees. In addition, the MAE for HLEN and HWID cross-section measurements ranged from 0.27 to 0.43 inch, where significant. DEPTH, however, had a large MAE range, 1.35 to 1.45 inches. Analyzing the predictor equations using the model testing samples showed that the correlations failed to be statistically significant ($\alpha < 0.01$) for the majority of AK and AKC internal features. For AK defects, only HWID and RAKE had significant correlation coefficients, 0.52 and 0.51, respectively, with surface features. With the AKC defects, HWID and DEPTH were the only internal features that had a significant correlation with the correlation model (correlation coefficient R=0.61 and R=0.80, respectively).

DISCUSSION

Overall, the strongest correlations, both model development and testing, occurred with the most severe defect types (OK, SK, and UK). These defects occurred most recently on the tree and have had the least time to be encapsulated or grown over. Thus, more detail about the surface indicator exists. Conversely, some of the weakest correlations that were discovered involved the least severe defect types (AK, AKC, LD, MD, HD). The adventitious knots/buds and the light and medium distortions were the oldest defects examined and had the longest time to encapsulate. Thus, less surface indicator existed for these defect types. A heavy distortion defect is at the point in the encapsulation process where an overgrown knot has made the transition to a distortion defect. More surface indicator detail exists for this type of distortion than the others, as evident in the predictive power of the HD feature models when compared to the MD and LD defect models. These results closely agree with those from the yellow-poplar defect study (Thomas 2008).

The results from this study indicate that most internal defects can be accurately estimated using external feature data. To date, yellow-poplar and red oak have been studied, resulting in the development of internal defect prediction models. These models will be further developed and tested using samples from additional sites. Models for additional hardwood species are in progress.

The goal of this research was to develop models capable of predicting internal defect features based on external defect characteristics. These models were developed to complement scanning and defect detection research that locates severe defects on hardwood stems (Thomas and Thomas 2011). Recent efforts at West Virginia University (WVU) have created a computer program (Lin et al. 2011) that generates sawing solutions that optimize recovery according to National Hardwood Lumber Association (NHLA) lumber grades, which use the external defect scan data and the predicted internal defect data from this model. As such, the prediction models allow the optimizer to know how deeply encapsulated a given defect is, how big it is, and how deep the defect penetrates the log. For example, the defect models allow the optimizer to know if a defect would be removed when a slab is sawn from the log. All of these research efforts are being pursued as an aid to hardwood sawing.

ACKNOWLEDGMENTS

The author would like to thank MeadWestvaco in Rupert, WV, and Robert Driscole at the WVU Experimental Forest for their assistance in sample collection.

LITERATURE CITED

Carpenter, R.D. 1950. **The identification and appraisal of log defects in southern hardwoods.** Presentation delivered at the Deep South Section – Forest Products Research Society Annual Meeting, Memphis, TN. Oct. 26, 1950.

Carpenter, R.D.; Sonderman, D.L.; Rast, E.D. 1989. **Defects in hardwood timber.** Agric. Handb. 678. Washington, DC: U.S. Department of Agriculture. 88 p**.**

Chang, S.J. 1992. **External and internal defect detection to optimize the cutting of hardwood logs and lumber.** Transferring technologies to the hardwood industry. Handb. 3. Beltsville, MD: U.S. Department of Commerce. 24 p.

Hyvärinen, M.J. 1976. **Measuring quality in standing trees – Depth of knot-free wood and gra**in **orientation under sugar maple bark distortions with underlying knots.** Ann Arbor, MI: University of Michigan. 142 p. Ph.D. dissertation.

Komsta, L. 2006. **Processing data for outliers.** R News. 6(2): 10-13.

Lemieux, H; Beaudoin, M; Zhang, S.Y. 2001. **Characterization and modeling of knots in black spruce (*Picea mariana*) logs.** Wood and Fiber Science. 33(3): 465-475.

Lin, W.; Wang, J.; Thomas, R.E. 2011. **A three-dimensional optimal sawing system for small sawmills in central Appalachia.** In: Fei, S., et al., eds. Proceedings, 17th central hardwood forest conference. Gen. Tech. Rep. NRS-P-78. Newtown Square, PA: U.S. Department of Agriculture, Forest Service, Northern Research Station: 67-76.

R Development Core Team. 2006. **R: A language and environment for statistical computing**. R Foundation for Statistical Computing, Vienna, Austria. ISBN 3-900051-07-0. Available at http://www.R-project.org. (Accessed March 1, 2012)

Shigo, A.L.; Larson, E.H. 1969. **A photo guide to the patterns of discoloration and decay in living northern hardwood trees**. Res. Pap. NE-127. Upper Darby, PA: U.S. Department of Agriculture, Forest Service, Northeastern Forest Experiment Station. 100 p.

Schultz, H. 1961. **Die beureilung der Qualitätsentwicklung junger** Bäum, Forstarchiv, XXXII (May 15, 1961). 97 p.

Steele, P.H.; Harless, T.E.G.; Wagner, F.G.; et al. 1994. **Increased lumber value from optimum orientation of internal defects with respect to sawing pattern in hardwood logs.** Forest Products Journal. 44(3): 69-72.

Thomas, L.; Thomas, R.E. 2011. **A graphical automated detection system to locate hardwood log surface defects using high-resolution three-dimensional laser scan data.** In: Fei, S., et al., eds. Proceedings, 17th central hardwood forest conference. Gen. Tech. Rep. NRS-P-78. Newtown Square, PA: U.S. Department of Agriculture, Forest Service, Northern Research Station: 92-101.

Thomas, R.E. 2008. **Predicting internal yellow-poplar log defect features using surface indicators.** Wood and Fiber Science. 40(1): 14-22.

Tuszynski, J. 2006. **caTools: Miscellaneous tools: I/O, moving window statistics, etc.** R package version 1.14. Available at http://cran.r-project.org/web/packages/caTools/caTools.pdf (Accessed April 15, 2013)